v. 1, n. 3, 2021

International Journal of Health Science

EFFECT OF BLOOD GLUCOSE LEVELS ON THE HSA-HYDRO-CHLOROTHIAZIDE INTERACTION - A SPECTRO-FLUORIMETRIC STUDY

Marilia Amável Gomes Soares
Postgraduation in Medical Sciences, Faculty of Medical Science, Rio de Janeiro State University
Rio de Janeiro, Brazil
http://lattes.cnpq.br/1584205887314033

Otávio Augusto Chaves
Institute of Chemistry, Federal Rural University of Rio de Janeiro
Rio de Janeiro, Brazil
http://lattes.cnpq.br/5839459732532799

Dari Cesarin-Sobrinho
Institute of Chemistry, Federal Rural University of Rio de Janeiro
Rio de Janeiro, Brazil
http://lattes.cnpq.br/5022515284689355

Dilson Silva
Postgraduation in Medical Sciences, Faculty of Medical Science, Rio de Janeiro State University
Rio de Janeiro, Brazil
http://lattes.cnpq.br/8363035335547588

Célia Martins Cortez
Postgraduation in Medical Sciences, Faculty of Medical Science, Rio de Janeiro State University
Rio de Janeiro, Brazil
http://lattes.cnpq.br/6107034183202542

Abstract: The interaction of HSA with hydrochlorothiazide in absence and presence of glucose was studied through UV-Vis absorption and fluorescence spectroscopy at 37 ºC. The interaction of a drug with human serum albumin influences its bioavailability and the high blood glucose level can promote the formation of glycation end products, and affect protein ability to transport drugs. To assess the glucose effect on the ability of hydrochlorothiazide to bind HSA, normoglycemic (80 mg glucose/dl) and hyperglycemic (320 mg glucose/dl) solutions were used. Competitive binding studies were performed using markers for Sudlow I (warfarin) and Sudlow III (digitoxin). Results showed good correlation of the observations made through the UV-Vis spectroscopy and the spectrofluorimetric measurements, concerning the association of ground state and the disturbance in the microenvironment around the aromatic amino acid residues. The fluorescence quenching of HSA by hydrochlorothiazide in the GLU absence and presence occurred by formation of complex drug-HSA. High glucose concentrations may decrease the number of available binding sites for drug in the IIA subdomain, probably due to albumin conformational change, making the binding of drug in the vicinity of residue Triptophan-214 difficult. Results suggest that a glycemic control is required to obtain an appropriate treatment with hydrochlorothiazide.
Keywords: Diabetes mellitus, glucose, hydrochlorothiazide drug, human serum albumin, spectroscopy.

INTRODUCTION

Diabetes mellitus (DM) is a chronic disease that has been a major threat to human health in recent decades, and is characterized by the high level of blood sugar resulting from the lack of insulin production or the insulin

resistence or both (Shrivastva et al., 2020). It can lead to premature deaths, as well as serious complications and disabilities, especially among younger populations in developing countries, including India and Brazil (Fu et al., 2020; Ramachandran et al., 2007). Projections for *2030* and *2040* indicate, respectively, 439 and 642 million people living with diabetes worldwide (Hajizadeh-Sharafabad et al., 2020).

Currently, the diagnosis of patients with DM is based on the blood glucose level after 8 hours of fasting. The values established by the Diabetes Association for the concentration of glucose (GLU) in the blood vary from 70 to 100 mg/dl, for normoglycemic patients, and above 125 mg/dl, for those considered diabetic (American Diabetes Association, 2003).

DM can cause dyslipidemia and hypertension, including macrovascular complications in the coronary arteries, as well as peripheral and cerebrovascular vascular diseases. In addition, microvascular complications related to retinopathy, nephropathy and neuropathy can also be found (Ramachandran et al., 2007; Ginsberg, 2000).

Since the main cause of morbidity in patients with DM is due to macro and microvascular complications, the risk of arterial hypertension is high, therefore, being the pressure control a great challenge for these patients (Chanda et al., 2009; Yeates et al. 2015). Several classes of drugs have been used to treat hypertension in patients with DM, such as beta-blockers, ACE inhibitors, calcium channel blockers, thiazide diuretics and others (Krum et al. 2003; Bertoluci et al., 2014).

The group of thiazide diuretics, as hydrochlorothiazide (HCTZ), has been used for the treatment of hypertension for more than 50 years. HCTZ is the drug of choice for the initial treatment of hypertensive diabetic patients, since it reduces blood volume, leading to a decrease in vascular resistance and a consequent reduction in blood pressure, and is frequently introduced into therapy when other classes of drugs do not are tolerated (Lin et al. 2016; Scheen, 2018; American Diabetes Association, 2004).

However, some clinical studies do not recommend the use of HCTZ for hipertensive patients, diabetic or non-diabetic, due to the possility of GLU induce tolerance and cause adverse metabolic effects, promoting clinical complications (Krum et al. 2003; Bertoluci et al., 2014; Lin et al. 2016; Scheen, 2018; American Diabetes Association, 2004; Mazzuchello et al. 2016; Rosendorff, 2011; Ribeiro, 2014). But, there are clinical studies indicating low impact on the alteration of fasting GLU, and they not support the idea of effects on glycemic control and lipid profile (Hall et al., 2020). Others suggest that the adverse effects caused by HCTZ may be associated to prolonged use and high doses (> 50 mg/day) (Carter & Basile, 2005; Burniera et al., 2019).

HCTZ continues to be used, mainly in low doses (<25 mg/day) and, according to the VI Brazilian Guidelines on Hypertension, published in 2010, thiazide diuretics reduce morbidity and mortality (Ribeiro, 2014). In general, the published works present a large number of data showing the positive and negative use of HCTZ, but they do not clarify the reason that this medication causes or not the possible adverse effects mentioned (Carter & Basile, 2005; Burniera et al. 2019).

The interaction of a drug with blood components influences its bioavailability and can affect the function of several biomolecules, endogens and exogens (Tamura et al., 1990). Human serum albumin (HSA) is the main transport protein in blood, comprising 60% of the total protein, and it plays an effective role in the balance of plasmatic concentrations

of drugs and their metabolites, influencing significantly on their absorption, distribution, elimination and clinical effects (Silva et al. 2004a; 2004b). In this way, the study on the interaction of HCTZ with albumin becomes relevant, especially to verify how hyperglicemia influence on this interaction. It is important to highlight that the increase in the human blood GLU can promote the formation of advanced glycation end products, which may cause structural perturbation on the blood proteins and affect their ability to transport drugs (Brownlee, 2005).

Spectrofluorimetry have been widely used in these types of studies, especially fluorescence quenching measurement. HSA containn 585 amino acids residues (molecular weight of 66.5 kDa) distributed into three main domains (I, II and III). These domains are subdivided into A and B, have helical form and cross-linked extensively through disulfide bridges. Tryptophan (Trp) residue at position 214 in subdomain IIA is the main responsible for the intrinsic fluorescence of HSA. (Morais-Coura, et al. 2021; Cortez et al., 2012; Silva et al., 2013; Simmons et al., 2014)

The present work describes the results of a study on the interaction between HSA with GLU and HCTZ using UV-Vis absorption and steady-state fluorescence at 37 ºC. To assess the effect of GLU on the ability of HSA to bind HCTZ, normoglycemic (80 mg GLU/dl blood) and hyperglycemic (320 mg GLU/dl blood) concentrations was used.

MATERIAL AND METHODS

MATERIAL

HSA, D - (+) - glucose, phosphate buffer solution (PBS) and HCTZ (6-chloro-3-3,4-dihydro-2H-1,2,4-benzothiadiazine-7-sulfonamide1,1-dioxide) were purchased from Sigma-Aldrich Chemical Company, St. Louis, USA and used without further purification. Figure 1 shows the chemical structure of HCTZ. In all experiments, it was used purified water from a Millipore Milli-Q system (company Merck KGaA, Darmstadt, Germany). Methanol (spectroscopic grade) was obtained from Vetec, Química Fina Ltda, Rio de Janeiro, Brazil.

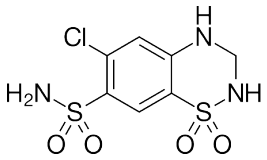

Figure 1. Chemical structure for hydrochlorothiazide (HCTZ).

Steady-state fluorescence spectra were obtained on a Jasco J-815 spectrophotometer coupled to a Jasco PFD425S15F thermostatic cuvette door (Jasco Easton, MD, USA) with 0.1 ºC accuracy. The UV-Vis spectra were obtained using a Varioskan LUX Multimode cuvette reader with an internal temperature control system (Thermo Fisher Scientific, Oregon, USA). For synchronous fluorescence measurement was used a Xe900 fluorometer model from Edinburgh Instruments (Edinburgh, UK). Spectroscopic measurements used a 1.0 cm quartz cells, and the corresponding background correction was carried out.

METHODS

As the purpose of the work was to simulate the behavior of GLU in the human body upon HCTZ administration, experiments were performed at 37 ºC, because of its proximity to physiological temperature, and using solutions of HSA (pure or not) 10^{-5} M in PBS at pH 7.4.

UV-Vis Measurements

The UV-Vis absorption spectra were registred from 200 to 500 nm wavelength, for five different solutions: (1) pure HSA solution (10^{-5} M in PBS); (2) HCTZ solution ($1.34x10^{-5}$ M in PBS); (3) HSA and HCTZ

solution (HSA-HCTZ, 10^{-5} M and 1.34 x10^{-5} M); (4) HSA, GLU and HCTZ (HSA-GLU-HCTZ) solution with 80 mg/dl of GLU; and (5) HSA-GLU-HCTZ solution with 320 mg/dl of GLU. These GLU concentrations are within of glycemic ranges considered normal (from 70 to 100 mg/dl) and diabetic blood glucose (high than 126 mg/dl) (Pereg et al., 2010). Thus, here, ***normoglycemic HSA solution*** refers HSA solution containing 80 mg/dl of GLU, and ***hyperglycemic HSA solution*** refers HSA solution containing 320 mg/dl of GLU.

Steady-State Fluorescence Measurements

The steady-state fluorescence emission spectra were registred from 310 to 400 nm, using excitation wavelength (λ_{exc}) of 295 nm.

Fluorescence Spectra were registered for addition of HCTZ (0.17; 0.34; 0.50; 0.67; 0.84; 1.00; 1.17 and 1.34 x10^{-5} M) in solutions of (1) pure HSA solution (10^{-5} M in PBS); (2) normoglycemic HSA solution; and (3) hyperglycemic HSA solution. HTCZ was added from concentrated stock solutions so that volume increment was negligible.

Since HCTZ showed significant absorption at the excitation and emission wavelengths (295 and 340 nm, respectively), the inner filter correction was applied to the steady-state fluorescence data, according to equation: $F_{co} = F_{ob}10^{[(A_{ex}+A_{em})/2]}$, where F_{co} and F_{ob} are the corrected and observed fluorescence intensity values, respectively; A_{ex} and A_{em} are the absorbance values for ligand at excitation (λ_{exc} = 295 nm: ε = 3271/cm.M in PBS) and emission wavelength (λ_{em} = 340: ε = 511.4 / cm.M in PBS).

Graphs were plotted according to the equations (Lakowicz, 2006):

$$\frac{F_0}{F} = 1 + k_q \tau_0 [Q] = 1 + K_{SV}[Q] \quad (a),$$

$$k_q = \frac{K_{SV}}{\tau_0} \quad (b),$$

where F_0 and F are the steady-state fluorescence intensities of HSA in the absence and presence of ligand, respectively. The K_{sv}, k_q, τ_o and (Q) are the Stern-Volmer quenching constant, bimolecular quenching rate, fluorescence lifetime constant of pure HSA (5.98 ± 0.16 x 10^{-9} s) and ligand concentration, respectively.

The values of apparent binding constant (K_b) and the binding site classes (n) were determined by using the equation (Lakowicz, 2006):

$$log\left(\frac{F_0 - F}{F}\right) = logK_b + n.log[Q]. \quad (2)$$

SYNCHRONOUS FLUORESCENCE EXPERIMENTS

Synchronous fluorescence (SF) of pure HSA and HSA solutions containing 80 or 320 mg/dl GLU were registred for each addition of HCTZ (0.17; 0.34; 0.50; 0.67; 0.84; 1.00; 1.17 and 1.34 x10^{-5} M), defining, $\Delta\lambda_{EE}$ = 15 nm ($\Delta\lambda_{EE}$ = excitation and emission wavelengths) and $\Delta\lambda_{EE}$ = 60 nm for tyrosine (Tyr) and Trp residues, respectively, in the 240-320 nm range, at room temperature.

COMPETITIVE BINDING STUDIES

Competitive binding studies were performed using markers for Sudlow I and Sudlow III sites: warfarin and digitoxin, respectively. HSA-marker solution and normoglycemic and hyperglycemic HSA-marker solutions were titrated with HCTZ. For each data point, the internal filter was corrected. The values of apparent binding constant (K_b) and the binding site classes (n) were determined by using Eq. 2.

RESULTS

Figure 2 shows the UV-Vis absorption spectra for solutions of 10^{-5} M HSA (black), 1.34 x10^{-5} M HCTZ (blue), and HSA

containing HCTZ (HSA-HCTZ, red) in PBS, pH = 7.4, as well as the difference between the absorption spectra (green) of HSA-HCTZ and pure HCTZ solutions. The detail on this figure highlights the 250-300 nm region of spectra. The increase in the level of UV-Vis absorption caused by the addition of HCTZ to the HSA solution is clear, as well as the shift towards blue (to the left) of the maximum UV absorption, compared to the spectrum of pure HSA.

In Figures 3, the UV-Vis absorption spectra for solutions 10^{-5} M HSA (black), GLU containing 1.34 x10^{-5} M HCTZ (GLU-HCTZ, blue) and HSA containing GLU and HCTZ (HSA-GLU-HCTZ, red) in PBS to pH=7.4. The green spectrum refers to the difference in UV-Vis absorption of HSA-GLU-HCTZ and GLU-HCTZ solutions. Figure 3*a* shows the spectra for the normoglycemic solution (GLU = 80 mg / dl) and Figure 3*b* shows the spectral behavior for the hyperglycemic solution (GLU = 320 mg / dl). The detail on these figures also highlights the 250-300 nm regions. Comparing these spectra, it is clearly observed that the addition of HCTZ to the HSA solution containing GLU also causes blue shifts of the UV absorption maximum, in relation to the spectrum of pure HSA.

Figure 4*a* shows the fluorescence spectra of HCTZ-titrated HSA (from 1.7 to 13.4 x10^{-5} M) at 37°C. Analysis of this figure shows that the gradual quenching of HSA fluorescence is followed by a slight red shift (right shift) in the fluorescence spectrum. The excitation wavelength was 295 nm and the emission spectra were recorded from 300 to 400 nm. In Figures 4*b* and 4*c* are the fluorescence spectra resulting from titration of HSA normo and hyperglycemic solutions by HCTZ, respectively. Comparing the spectra in these two figures, it can be seen that the fluorescence quenching caused by HCTZ was more intense in the hyperglycemic than in the normoglucemic HSA solution.

Figure 5*a* presents the Stern-Volmer plots for the HSA-HCTZ interaction in the absence and presence of GLU (normo and hyperglycemic solutions) at 37°C. This figure evidences the linearity of the plots for drug interacting with pure and normoglycemic HSA solution, but the plot for the hyperglycemic HSA solution curves downwards with increasing HCTZ concentration. This behavior clearly not linear suggests that other sites for HCTZ opening when its concentration increases. To estimate Stern-Volmer constants, regions of low HCTZ concentrations were solely considered (detail on Figure 5*a*), where we can study the highest affinity interactions [Silva et al. 2004b). Figure 5*b* exhibits the plots log (F0-F)/F) versus log [Q] (Eq. 2).

The values corresponding to K_{SV} (Eq. 1*a*) and k_q (Eq. 1*b*) for the interaction of HTCZ with HSA in the presence and absence of GLU, calculated for low titrant concentrations (detail Figure 5a), are shown in Table 1, as well as the K_b and n values (Eq. 2). It is important to note the small difference between the K_{SV} and K_b values for the interactions of HCTZ with pure and normoglycemic HSA, indicating that the presence of GLU does not significantly affect the quenching rate constant. However, important increases in K_{SV} values (from 1.38 to 2.88 x10^4 /M) and K_b (from 1.47 to 4.52 x104 /M) occurred for the drug interaction with hyperglycemic HSA. Furthermore, the value of *n* (number of binding site classes) decreases with increasing GLU concentration in the HSA solution, moving away from 1.

Figures 6*a* and 6*b* show the SF results of pure HSA solution titrated by HCTZ for $\Delta\lambda_{EE}$ =15 nm and $\Delta\lambda_{EE}$ = 60 nm, respectively. Figures 6*c* and 6*d* allow to compare the behavior of the fluorescence spectra of the hyperglycemic solution of HSA (GLU = 320 mg / dl) titrated by drug. Note that important redshift of the

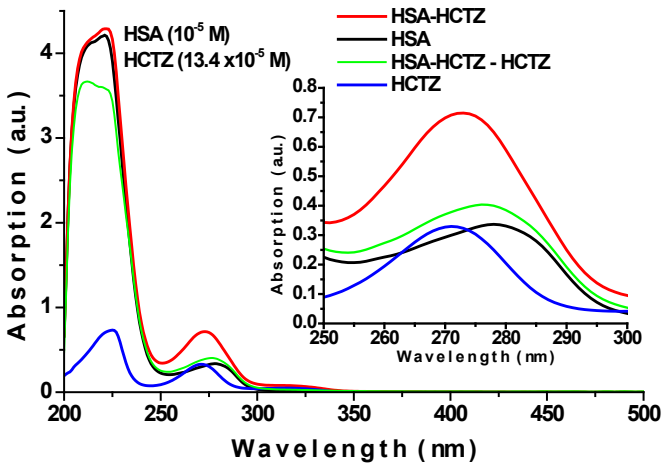

Figure 2. UV-Vis spectra for HSA (black) and HCTZ (blue) HSA-HCTZ (red) in PBS solution (pH = 7.4), and mathematical subtraction (HSA-HCTZ) – (HCTZ) (green). [HSA] = 10^{-5} M, [HCTZ] = 1.34 x10^{-5} M.

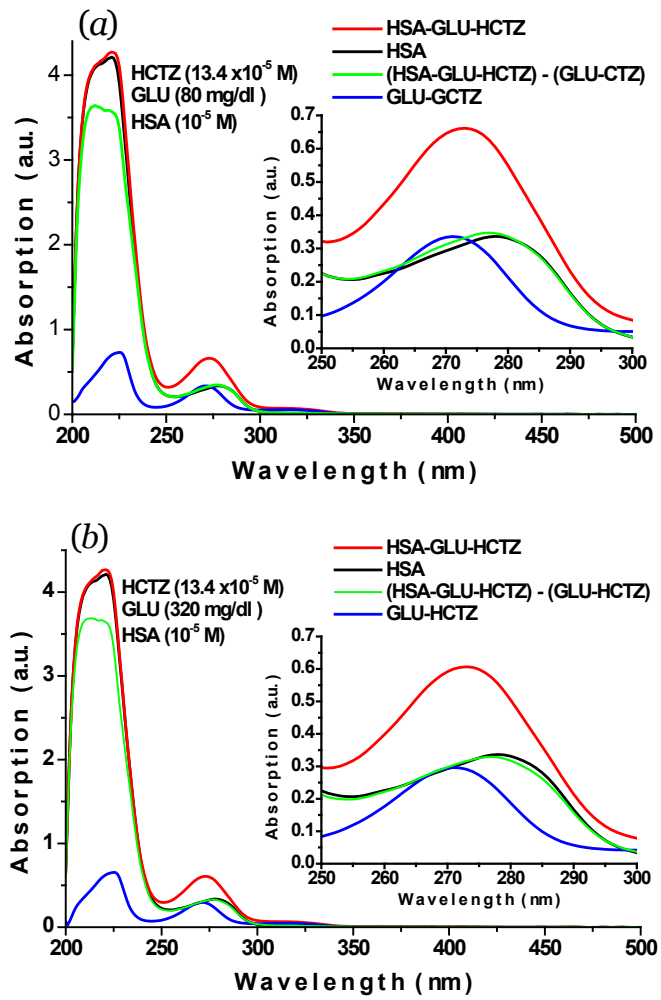

Figure 3. UV-Vis spectra for HSA (black), GLU-HCTZ (blue) and HSA-GLU-HCTZ (red) in PBS solution, PH 7.4. In (*a*) [GLU] = 80 mg/dl and (*b*) [GLU] = 320 mg/dl; mathematical subtraction (HSA-GLU-HCTZ) - (GLU-HCTZ) in green. [HSA] = 10^{-5} M, [HCTZ] = 1.34 x10^{-5} M.

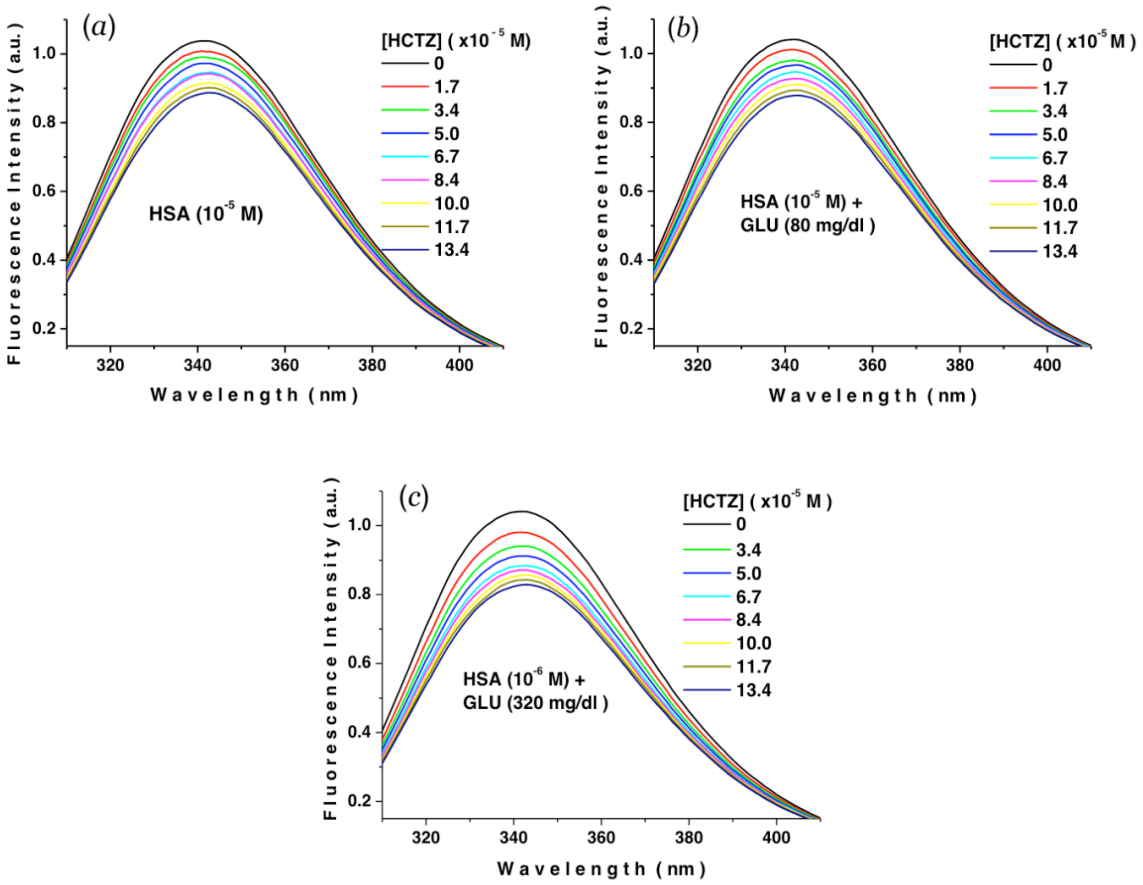

Figure 4. Steady-state fluorescence spectra of (*a*) HSA-HCTZ, (*b*) HSA-GLU-HCTZ for [GLU] = 80 mg/dl, and (*c*) HSA-GLU-HCTZ for [GLU] = 320 mg/dl, at 37 °C and pH = 7.4 (λ_{exc} = 295 nm). [HSA] = 10^{-5} M.

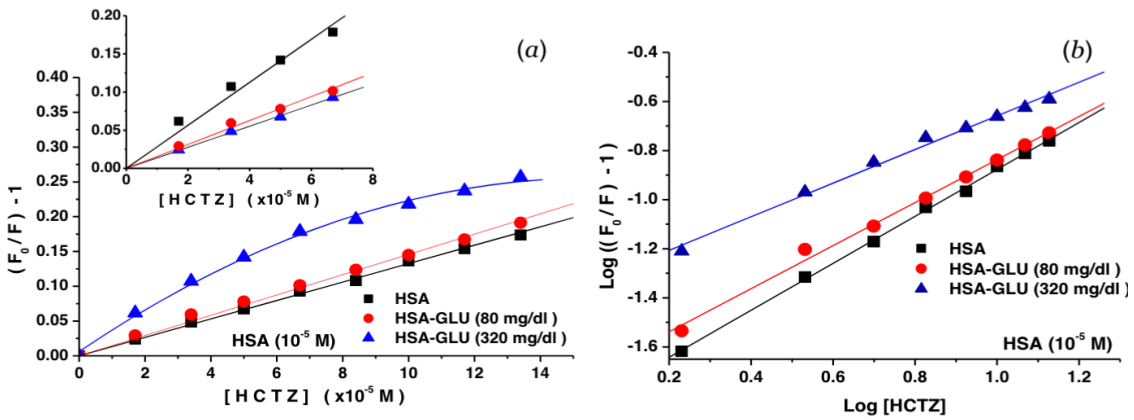

Figure 5. (*a*) Stern–Volmer plots for the interactions HSA-HCTZ in absence and presence of GLU at 37 °C; (*b*) Double logarithmic plots for the interaction HSA-HCTZ in absence and presence of GLU at 37 °C. [HSA] = 10^{-5} M, [Glucose] = 80 and 320 mg/dl, pH = 7.4 (λ_{exc} = 295 nm).

Sample	K_{SV} (x10^4/M)	k_q (x10^{12}/M.s)	K_b (x10^4/M)	n
HSA-HCTZ	1.38 ± 0.01	2.12	1.47 ± 0.01	0.96 ±0.02
HSA-GLU-HCTZ[1]	1.57 ± 0.03	2.19	1.87 ± 0.01	0.88 ±0.03
HSA-GLU-HCTZ[2]	2.82 ± 0.09	2.17	4.53 ± 0.02	0.68 ±0.01

[1]80 mg/dl and [2]320 mg/dl of glucose (GLU).

Table 1. Values of K_{SV}, k_q, K_b and n for interaction HSA-HCTZ, in the absence and presence of GLU, at 37 ºC.

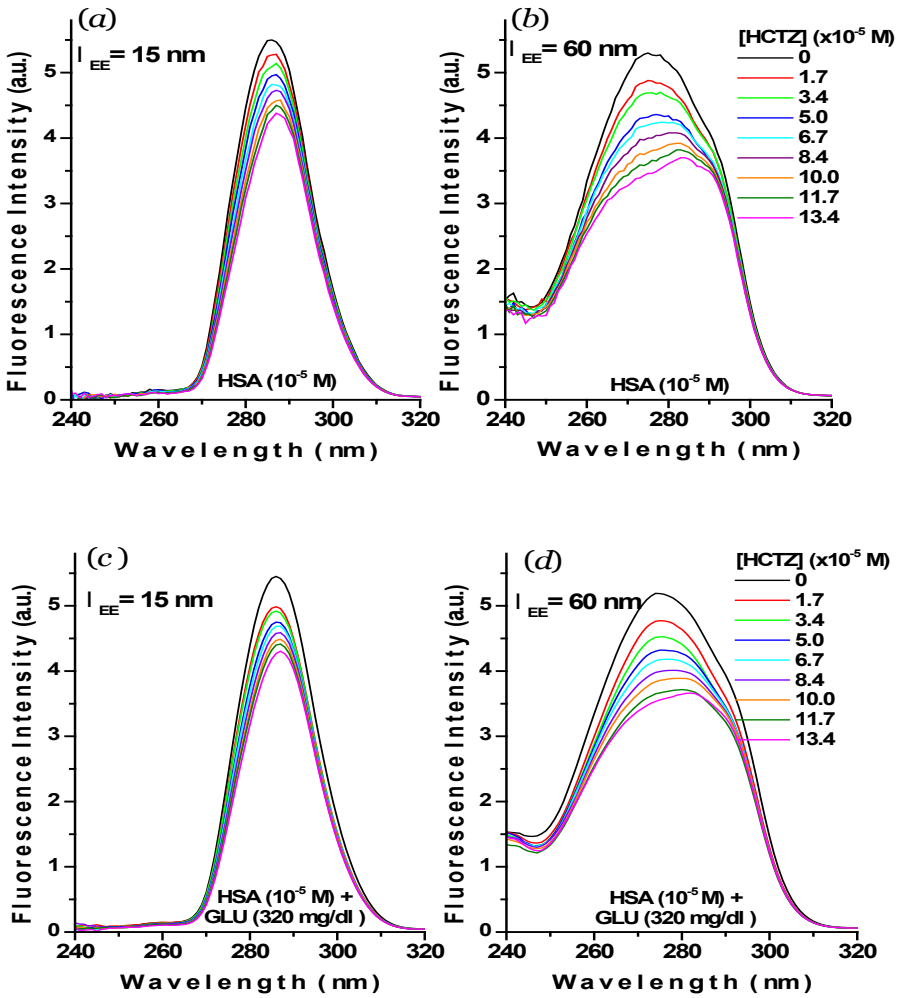

Figure 6. Synchronous fluorescence spectrum for: (*a*) HSA-HCTZ, $\Delta\lambda_{EE}$ = 15 nm; (*b*) HSA-HCTZ, $\Delta\lambda_{EE}$= 60 nm; (*c*) HSA-GLU-HCTZ, $\Delta\lambda_{EE}$ = 15 nm; and (*d*) HSA-GLU-HCTZ, $\Delta\lambda_{EE}$= 60 nm ($\Delta\lambda_{EE}$ = excitation and emission wavelengths), at 37 ºC and pH = 7.4 (λ_{exc} = 295 nm). [HSA] = 10^{-5} M, [Glucose] = 320 mg/dl.

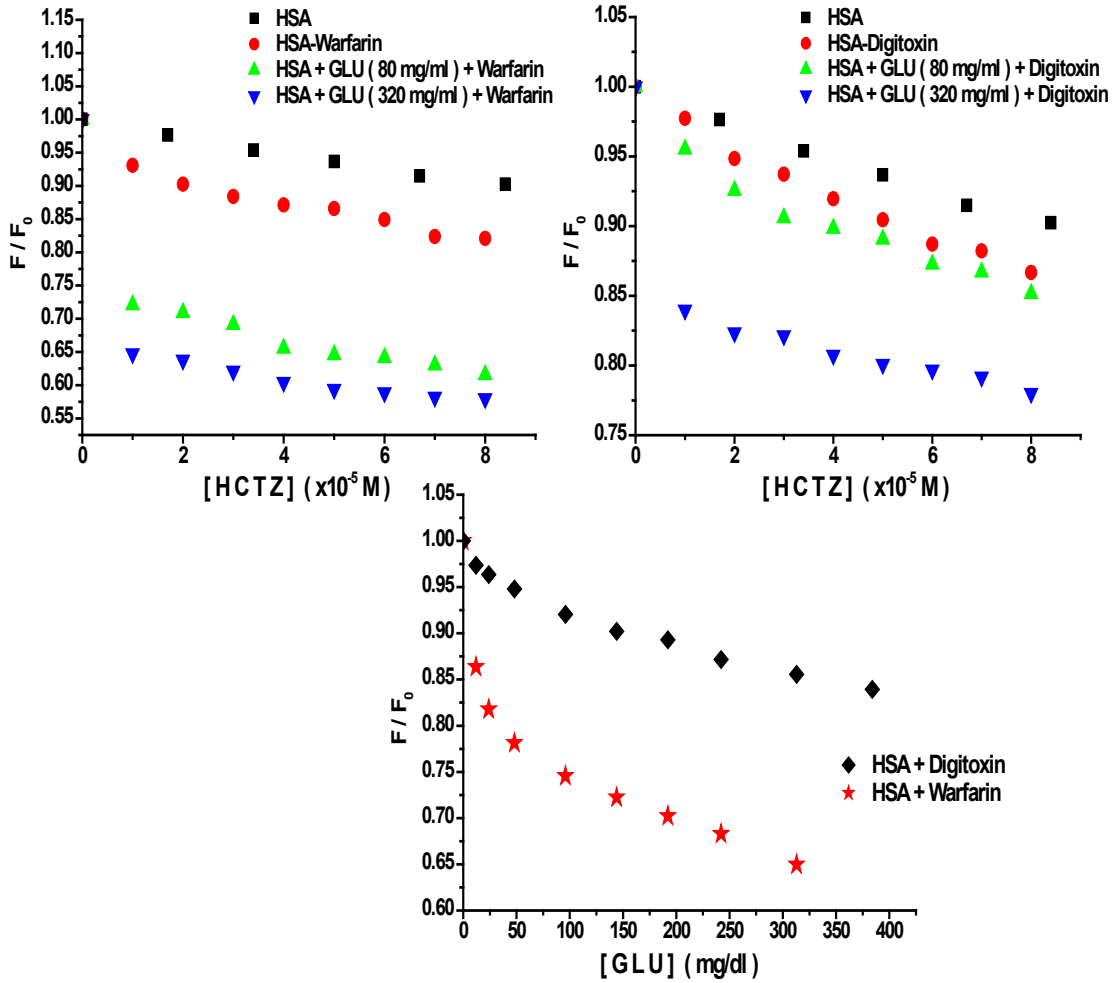

Figure 7. Normalized quenching curves for (*a*) pure HSA titrated by HCTZ, (*b*) normoglycemic and hyperglycemic HSA solutions titrated by HCTZ in presence of warfarin, (*c*) HSA titrated by GLU in presence of warfarin and digitoxin, at 37 °C and pH = 7.4. [HSA] = 10^{-5} M (λ_{exc} = 295 nm).

fluorescent emission maximum occurs with the HCTZ concentration increase for $\Delta\lambda_{EE}$ =60 nm for pure HSA and hyperglycemic HSA solutions. This wavelength refers to changes in the environment close to Trp (37).

Figs. 7*a* shows normalized quenching curves of pure HSA titrated by HCTZ in absense and presence de warfarin at 37°C, as well as normo and hyperglycemic HSA solutions titrated by HCTZ in presence of warfarin. Fig. 7*b* presents the same of Fig. 7*a*, but for digitoxin, and Fig. 7*c* allows to comparing the normalized quenching curves of HSA titrated by HCTZ in presence of the both markers of sites, warfarin and digitoxin.

It is possible observe in Fig.7*a* that warfarin increased the level of fluorescence HSA quenching caused by HCTZ, which still became more intense with the concentration increase of GLU in solution. At 1:1 molar ratio of HCTZ/HSA, HCTZ quenches about 6.3% of HSA fluorescence. In presence of warfarin, the fluorescence quenching falled to about 13.4%, 35.4% and 40.6% for HSA-HCTZ and normo and hyperglycemic HSA-CHTZ-GLU, respectively. In Fig. 7*b* we can be seen that digitoxin effect on fluorescence was lower than that warfarin. Comparing to fluoresecence quenching caused by HCTZ on pure HSA, at 1:1 molar ratio of HCTZ/HSA, quenching increased 9.54% in presence of digitoxin, and increased of 10.94% and 19.90% with adition of GLU, respectively, 80 mg/dl GLU and 320 mg/dl of GLU. Figure 7c evidences that the quenching of GLU on HSA was more intense than that digitoxin. At first adition of GLU to HSA 10^{-5} M, fluorescence was rediced of 13.63% and 2.63% in presence warfarin and digitoxin, respectively.

DISCUSSION

Absorption spectroscopy UV-Vis is a direct method that has been frequently applied to explore structural changes and the complex formation between a protein and small molecules (Suryawanshi et al., 2016). HSA presents maximum absorbance peaks at 222 and 280 nm, attributed to n-π^* and π-π^* transitions, respectively, which are associated with the aromatic amino acid residues: Trp, Phe (phenylalanine) and Tyr (Lakowicz, 2006; Shi et al., 2016; Zhou et al., 2019). HCTZ exhibits maximum absorbance peaks at 225 and 269 nm, attributed to the π-π^* and n-π^* transitions of the aromatic ring and sulfonamide groups, respectively.

After the addition of HCTZ to the HSA solution, a significant blue shift is observed in albumin spectrum (Figure 2), indicating a disturbance in the microenvironments around the aromatic amino acid residues due to the HSA-HCTZ interaction (Naik et al., 2015; Zhang et alo,. 2013; Roy et al., 2015). In the presence of GLU (Figures 3), the addition of HCTZ to normoglycemic (Figure 3*a*) and hyperglycemic (Figure 3*b*) HSA solutions also generated blue shifts in the respective UV-Vis absorption spectra, indicating the same disturbance trend in the aromatic microenvironments. Furthermore, comparing the GLU-HCTZ interaction spectra in Figures 3*a* and 3*b* HSA, it is possible to observe at normal GLU level a slight hyperchromic effect comparing to the hyperglycemic level. These results suggest a decreasing in the HSA capacity to bind HCTZ in hyperglycemic state.

STEADY-STATE FLUORESCENCE ANALYSIS

The HSA fluorescence intensity gradually decreases with increasing concentration of HCTZ (Figure 4*a*) and spectral changes suggest the presence of a primary binding site for HCTZ near or within the IIA subdomain, where residue Trp-214 is located, in addition a possible proteic conformational change affecting the microenvironment around that residuo (Zhu et al., 2007; Stan et al., 2009).

It is known that the main HSA binding sites for drugs are located in hydrophobic cavities in the IIA and IIIA subdomains, where the Sudlow I and Sudlow II sites are located, respectively, but the presence of drug sites in the IB subdomain have already been identified (Fragoso et al., 2016; Fragoso et al., 2012). Anionic heterocyclic compounds of large molecular size bind especially in the site Sudlow I, located in subdomain IIA. The site Sudlow II (in subdomain IIIA) presents higher affinity to aromatic carboxylic drugs in therapeutic concentration (Morais-Coura et al., 2021). Hydrophobic and electrostatic interactions, as well as steric factors, play an essential role in determining the affinity and specificity of ligand binding at these sites (Ricciardi et al., 2020; Ermakova et al., 2020).

The quenching of HSA fluorescence by HCTZ became more intense with the increase of GLU concentration (Figures 4). The shift of the fluorescence maximum of HSA (Figure 4*a*) upon addition of HCTZ is opposite to that observed in the UV-Vis spectra (Figure 2), and it is important to remember that these result from different phenomena. The UV-visible absorption involves several amino acids present in the protein structure, while the fluorescence spectra concern the intrinsec fluorescence due to the residue Trp-214, since the l_{exc} = 295 (Lakowicz, 2006).

A slight redshift (Dl ~ 3 nm) in the fluorescence maximum of normo and hyperglycemic HSA solutions titrated by HCTZ (Figures 4*b* and 4*c*) is indicating that even in the presence of GLU, HCTZ can still interact in the IIA subdomain, causing some conformational change in this region (Silva et al., 2004b; Liang et al., 2020; Cheng et al., 2013).

No significant difference is observed in Table 1 between the K_{SV} and K_q values for HCTZ interactions with HSA in the absence and presence of 80 mg/dl GLU, indicating that the ability of HCTZ to quench HSA fluorescence is not significantly influenced in normoglycemic conditions. But the same cannot be said for the HCTZ-HSA interaction for the hyperglycemic condition. In this condition, the values of KSV and Kq were about 2.1 and 1.81 times higher than in the absence and presence of 80 mg/dl of GLU, respectively, confirming the interference of the glycemic level in the drug-HSA interaction.

Values obtained for k_q are of the order of 10^{12} /M.s, three orders of magnitude higher than the limiting constant of the diffusion rate in the water (k_{dif} ~ 7.40 x10^9 /M.s at 25 ºC, according to the Smoluchowski-Stokes Einstein Theory) (Montalti et al., 2006). This suggests that fluorescence quenching by HSA-HCTZ interaction, in the absence and presence of GLU, is mainly due to a static process, and results from UV-vis measurements confirm it. Thus, HCTZ binds to HSA by forming complex.

It is know that quenching may result from various processes such as energy transfer, excited state reactions, ground-state complex formation and collisional processes. Collisional or dynamic quenching is due to collisions between the quencher and fluorophore. In static quenching there is ground-state complex formation between the quencher and fluorophore, and significant change in the UV-Vis absorption spectrum can be observed (Lakowicz, 2006).

The K_b value for HSA-HCTZ is on the order of 10^4 /M (Table 1), indicating a moderate binding capacity of HCTZ to serum albumin at 37°C, in the absence and presence of GLU (Yan et al., 2015; Chaves et al., 2016).

In hyperglycemic condition, the K_b value estimated from steady state fluorescence quenching for HSA-HCTZ increased in relation to the two other conditions tested (absence of GLU and normoglycemia), maintaining the order of magnitude. But the

International Journal of Health Science ISSN 2764-0159 DOI 10.22533/at.ed.1592120104

value of n (n»1) estimated for interatyion HCTZ-HSA in absence of GLU suggests the existence of only one class of binding site for HCTZ in HSA at 37 °C, the primary binding site probably being located in the IIA subdomain, where is found the amino acid residue Trp-214.

However, increasing the GLU concentration in the HSA solution decreases the value of n. This suggests that hyperglycemic concentrations of GLU may disturb the albumin structure and decrease the number of sites available for the drug in the vicinity of Trp. In high concentration, GLU can adsorb on the protein surface, decreasing the accessibility of HCTZ to the binding site (Naveenraj & Anandan, 2013).

SYNCHRONOUS FLUORESCENCE ANALYSIS

Synchronous fluorescence spectroscopy (SF) is a fluorescence technique using difference between the excitation and emission wavelengths ($\Delta\lambda_{EE}$) of 15 and 60 nm, which allows to check changes in the environment close to Tyr and Trp, respectively (Lakowicz, 2006).

Analysis of the results from SF shows that the HSA fluorescence quenching with the increase of the HCTZ concentration for $\Delta\lambda_{EE}$=15 nm (Figure 6*a*) was not accompanied by a visible change in the maximum fluorescence emission. This is indicative that microenvironments around Tyr residues were not affected by the presence of drug. But, the same cannot be considered for residue Trp-214, since a visible red shift in the emission maximum, shown in Figure 6*b*, supports the occurrence of change in albumin conformation due to the HSA-HCTZ interaction for $\Delta\lambda_{EE}$ = 60 nm (Sudlow et al., 1976).

SF also showed that for hyperglycemic HSA solution there was no significant change in the fluorescent emission maximum with addition of HCTZ that might indicate alteration in the environment around tyrosine residues (Figure 6*c*). But the spectral alteration observed in Figure 6*d* reflets an importante change around of Trp-214.

The results from SF analysis are in agreement with those obtained from the UV-Vis spectra (Figures. 2 and 3). These suggest that even in the presence of GLU, the environment around the Trp-214 residue can undergo changes in its hydrophobicity.

COMPETITIVE BINDING

The quenching capacity estimated for the HSA-HCTZ interaction increased (Figure 7*a*) for the presence of both, warfarin and digitoxin. In the first case, the observed increase in quenching was 7.1% (from 6.3% to 13.4%), and in the second, the increase was 3.2% (Figure 7*b*), for the 1:1 molar ratio HCTZ/HSA. These increases were expanded in the presence of GLU and warfarin, as HSA fluorescence quenching by HCTZ increase in was 29.1% (from 6.3% to 35.4%), for the normoglycamic solution, and 34.3% (from 6.3% to 40.6 %) for hyperglycemic. It is known that the displacement of the ligand from its binding site in HSA by site markers may generate fluorescence quenching (Tan et al., 2019; Sun et al., 2016).

In the case of digitoxin, the increase was 1.4% (from 9.5% to 19.9%). The titration of HSA with GLU in the presence of site markers (Fig. 7*c*) showed that the quenching capacity of the fluorescence of this carbohydrate was important in the presence of warfarin and digitoxin (68% and 53%, respectively, for GLU 12 mg/dl). Such results suggest that both HCTZ and GLU compete with warfarin present in Sudlow's site I (IIA subdomain) of HSA, suggesting the existence of binding sites for both in the region where Trp-214 is located. However, local site III (for digitoxin) can

also accommodate these ligands, but to a lesser extent.

Therefore, the increase in HCTZ concentration appears to have increased the competitive ability of HCTZ by binding sites, and it ends up binding to sites in the IIIA subdomain. These data confirm the results shown in steady-state fluorescence quenching. Those results evidence the existence of a primary binding site for HCTZ in the IIA subdomain, and that increasing the GLU concentration must decrease the value of *n*. Therefore, the presence of GLU disturbs the interaction of HCTZ with HSA in the environment around residue Trp-214.

CONCLUSION

The analysis of the results shows the existence of a good correlation between the observations made through the UV-Vis and spectrofluorimetric measurements for the HSA-HCTZ interaction in normoglycemic (GLU=80 mg/dl) and hyperglycemic (GLU= 320 mg/dl) solutions, in relation to the association of ground state and the disturbance in the microenvironment around the aromatic amino acid residues, mainly for the hyperglycemic state.

The K_{SV} values indicate that the increase in GLU concentration does not affect the quenching capacity of HCTZ on HSA fluorescence, and k_q values are three orders of magnitude greater than k_{dif}. This confirms that fluorescence quenching by HSA-HCTZ interaction in the absence and presence of GLU occurs by the formation of a drug-HSA complex.

The binding constant (K_b) values obtained by the double logarithm approximation suggest an increase in the binding strength of HCTZ with albumin with increasing GLU concentration. However, the increase in K_b was accompanied by a decrease in the number of available sites (n) for drug binding in the IIA subdomain, making the HCTZ-HSA interaction in the vicinity of residue Trp-214 more difficult, probably due to albumin conformational change.

HCTZ has the ability to compete with warfarin and digitoxin by binding sites. At lower concentrations, the binding site is close to residue Trp-214 (where is warfarin binding site), but for high glycemic indices increase (320 mg/dl), HCTZ it ends up binding to sites in the IIIA subdomain (where is digitoxin binding site).

Results suggest that the need of a glycemic control in the human bloodstream to obtain the appropriate pharmacotherapeutic treatment at use the commercial drug HCTZ.

ACKNOWLEDGEMENTS

The authors would like to acknowledge the Brazilian agencies for the finantial support from Coordenação de Aperfeiçoamento de Pessoal de Nível Superior (CAPES), Conselho Nacional de Desenvolvimento Científico e Tecnológico (CNPq), and Fundação de Amparo à Pesquisa do Estado do Rio de Janeiro (FAPERJ), and Professor Frederico Alan de Oliveira Cruz (Department of Physics - UFRRJ) for the support in the first discussion of the experimental data.

INDIVIDUAL CONTRIBUTIONS

Soares M.A.S., Cortez C.M. and Silva D. idealized the study and wrote the paper. Gomes M.A.S and Cesarin-Sobrinho D. conducted the experiment procedures. Chaves O.A. participated of experimental data analysis. All authors participated in the final review of the manuscript, discussing the results and commenting on the conclusions.

CONFLICTS OF INTEREST

The authors declare no conflict of interest.

REFERENCES

American Diabetes Association (2003). Clinical Practice Recommendations. Report of the Expert Committee on the Diagnosis and Classification of Diabetes Mellitus. **Diabetes Care**, 26, s5-s20.

American Diabetes Association (2004). **Standards of Medical Care in Diabetes**, Diabetes Care, 27, s15-s35.

Bertoluci, M.C., Pimazoni-Netto, A., Pires, A.C., Pesaro, A.E., Schaan, B.D., Caramelli, B., Polanczyk, C.A., Júnior, C.V.S., Gualandro, D.M., Malerbi, D.A., Moriguchi, E., Borelli, F.A.O., Salles, J.E.N., Júnior, J.M., Rohde, L.E., Canani, L.H., Cesar, L.A.M., Tambascia, M., Zanella, M.T., Gus, M., Scheffel, R.S., & Santos, R.D. (2014). Diabetes and cardiovascular disease: from evidence to clinical practice – position statement 2014 of Brazilian Diabetes Society. **Diabetol Metab,** 602, 20, 58.

Brownlee, M. (2005). The pathobiology of diabetic complications. A unifying mechanism. **Diabetes**, 56, 1615-25.

Burniera, M., Bakrisc, G., & Williams, B. (2019). Redefining diuretics use in hypertension: why select a thiazide-like diuretic? **J. Hypert**., 37, 1574–1586.

Carter, B.L., & Basile, J. (2005). Development of diabetes with thiazide diuretics: The potassium issue. **J Clin Hypert**, 7, 638-640.

Chanda, R., & Fenves, A.Z. (2009). Hypertension in patients with chronic kidney disease. **Curr Hypertens Rep**, 11, 329-336.

Chaves, O.A., Jesus, C.S.H., Cruz, P.F., Sant'Anna, C.M.R., Brito, R.M.M., & Serpa, C. (2016). Evaluation by fluorescence, STD-NMR, docking and semi-empirical calculations of the o-NBA photo-acid interaction with BSA. **Spectrochim Acta A Mol Biomol Spectrosc**, 169, 175- 181.

Cheng, Z., Liu, R., & Jiang, X. (2013). Spectroscopic studies on the interaction between tetrandrine and two serum albumins by chemometrics methods. **Spectrochim Acta A Mol Biomol Spectrosc**, 115, 92–105.

Cortez, C.M., Silva D., Silva, C.M.C., & Missailidis S. (2012). Interactions of aptamers with sera albumins. **Spectrochim Acta A, Mol Biomol Spectrosc**, 95, 270-275.

Ermakova, E.A., Danilova, A.G., & Khairutdinov, B.I. (2020). Interaction of ceftriaxone and rutin with 638 human serum albumin. WaterLOGSY-NMR and molecular docking study. **J Mol Struct**, 639 1203, 127444.

Fragoso VM1, Silva D, Cruz FA, & Cortez CM. (2012). Risperidone interacts with serum albumin forming complex. **Environ Toxicol Pharmacol**, 33(2), 262-6.

Fragoso, V. M.S., de Morais Coura, C. P., Hoppe, L.Y., Soares, M.A.G., Silva, D., & Cortez, C.M. (2016). Binding of Sulpiride to Seric Albumins. **Int J Mol Sci**, 17(1), 59.

Fu, X., Nan, H., Liu, Z., Zhang, L., & Wang, X. (2020). Association of NAD+ ADP-ribosyltransferase 1 gene polymorphism with the development of neonatal diabetes mellitus. **J King Saud Univ. Sci**, 32, 2069-2073.

Ginsberg, H. (2014). Insulin resistance and cardiovascular disease. **J Clin Invest**, 2000, 106, 453-458.

Hajizadeh-Sharafabad, F., Varshosaz, P., Jafari-Vayghan, H., Alizadeh, M., & Maleki, V. (2020). Chamomile (Matricaria recutita L.) and diabetes mellitus, current knowledge and the way forward: A systematic review. **Complement Ther Med**, 48, 102284.

Hall, J.J., Eurich, D.T., Nagy, D., Tjosvold, L., & Gamble, J.-M. (2020). Thiazide diuretic–induced change in fasting plasma glucose: a meta-analysis of randomized clinical trials. **J Gen Int Med**, 35, 1849-1860.

Krum, H., Skiba, M., & Gilbert, R.E. (2003). Comparative metabolic effects of hydrochlorothiazide and indapamide in hypertensive diabetic patients. **Diabetic Medicine**, 20, 708–712.

Lakowicz, J.R. (2006). Principles of Fluorescence Spectroscopy, 3rd ed.; Springer: New York.

Liang, C.-Y., Pan, J., Bai, A.-M., & Hu, Y.-J. (2020). Insights into the interaction of human serum albumin and carbon dots: Hydrothermal synthesis and biophysical study. **Int J Biol Macrom**, 149, 1118-1129.

Lin, J.J., Chang, H.C., Ku, C.T., & Chen, H.Y. (2016). Hydrochlorothiazide hypertension treatment induced metabolic effects in type 2 diabetes: a meta-analysis of parallel-design RCTs. **Eur Rev Med Pharmacol Sci**, 20, 2926-2934.

Mazzuchello, F.R., Tuon, L., Simões, P.W., Mazon, J., Dagostin, V.S., Tomasi, C.D., Hoepers, N., Birol, I.V.B., & Ceretta, L.B. (2016). Knowledge, attitudes and adherence to treatment in individuals with hypertension and diabetes mellitus. **Mundo Saúde**, 40, 418-432.

Montalti, M., Credi, A., Prodi, L., & Gandolfi, M.T. (2006). **Handbook of Photochemistry**, 3rd 4ed., CRC 704 Press, Taylor e Francis, 2006.

Morais-Coura, C.P., Fragoso, V.M.S., Valdez, E.C.N., Paulino, E.T., Silva, D., & Cortez, C.M. (2021). Study on the interaction of three classical drugs used in psychiatry in albumin through spectrofluorimetric modeling. **Spectrochim Acta A, Mol Biomol Spectrosc** 255, 119638.

Naik, P.N., Nandibewoor, S.T., & Chimatadar, S.A. (2015). Non-covalent binding analysis of sulfamethoxazole to human serum albumin: Fluorescence spectroscopy, UV–vis, FT-IR, voltammetric and molecular modeling. **J Pharm Anal**, 5, 143–152.

Naveenraj, S., & Anandan, S. (2013). Binding of serum albumins with bioactive substances –Nanoparticles to drugs. **J Photochem Photobiol C**, 14, 53-71

Pereg, D., Elis, A., Neuman, Y., Mosseri, M., Lishner, M., & Hermoni, D. (2010). Cardiovascular risk in patients with fasting blood glucose levels within normal range original research. **Am J Cardiol**, 106, 1602-1605.

Ramachandran, A., Ramachandran, S., Snehalatha, C., Augustine, C., Murugesan, N., Viswanathan, V., Kapur, A., & Williams, R. (2007). Increasing expenditure on health care incurred by diabetic subjects in a developing country: a study from India. **Diabetes Care**, 30, 252–256.

Ribeiro, J.M. (2014). Hypertension guidelines: A view from Latin America. **J Clin Hypertens**, 16, 261-262.

Ricciardi, L., Guzzi, R., Rizzuti, B., Ionescu, A., Aiello, I., Ghedini, M., & Deda, M.L. (2020). Anionic 635 versus neutral Pt(II) complexes: The relevance of the charge for human serum albumin binding. **J Bioinorg Chem**, 206, 111024.

Rosendorff, C. (2014). Why are we still using hydrochlorothiazide? **J Clin Hypertens**, 13, 867-869.

Roy, D., Kumar, V., James, J., Shihabudeen, M.S., Kulshrestha, S., Goel, V., & Thirumurugan, K. (2015). Evidence that chemical chaperone 4-phenylbutyric acid binds to human serum albumin at fatty 672 acid binding sites. **PLoS ONE**, 10, e0133012.

Scheen, A.J. (2018). Type 2 Diabetes and Thiazide Diuretics. **Curr Diab Rep**, 18, 1-13

Shi, J.-H., Wang, Q., Pan, D.-Q., Liu, T.-T., & Jiang, M. (2016). Characterization of interactions of simvastatin, pravastatin, fluvastatin, and pitavastatin with bovine serum albumin: multiple spectroscopic and molecular docking. **J Biomol Struct Dyn**, 35, 7, 1529–1546.

Shrivastva, A., Phadnis, S., K.R. N, & Gore M. (2020) A study on knowledge and self-care practices about Diabetes Mellitus among patients with type 2 Diabetes Mellitus attending selected tertiary healthcare facilities in coastal Karnataka. **Clin Epidemiol Glob Health**, 2020, 8, 689-692.

Silva D, Cortez CM, & Louro SRW. (2004). Chlorpromazine interactions to sera albumins. A study by the quenching of fluorescence. **Spectrochim Acta Part A**, 60, 1215-1223

Silva D, Cortez CM, Silva CMC, & Missailidis S. (2013). A fluorescent spectroscopy and modelling analysis of anti-heparanase aptamers–serum protein interactions. **J Photochem Photobiol B: Biology**,12, 68-77.

Silva, D., Cortez, C.M., Cunha-Bastos, C., & Louro, S.R.W. (2004b). Methyl parathion interaction with human and bovine serum albumin. **Toxicol Lett**, 147(1):53-61.

Simmons SC, Jämsä H, Silva D, Cortez CM, McKenzie EA, Bitu CC, Salo S, Nurmenniemi S, Nyberg P, Risteli J, de Almeida CEB, Brenchley PEC, Salo T, & Missailidis S. (2014). Anti-Heparanase Aptamers as Potential Diagnostic and Therapeutic Agents for Oral Cancer. **PLoS ONE** 9(10): e96846.

Stan, D., Matei, I., Mihailescu, C., Savin, M., Matache, M., Hillebrand, M., & Baciu, I. (2009). Spectroscopic investigations of the binding interaction of a new indanedione derivative with human and bovine serum albumins. **Molecules**, 14, 1614-1626.

Sudlow, G., Birkett, D. J., & Wade, D. N. (1976). Further characterization of specific drug binding sites on human serum albumin. **Mol Pharm**, 12, 1052–1061.

Sun, M., Su, M., & Sun, H. (2016). **Int J Pharmaceit. Sci Res 7,** 1026-1034.

Suryawanshi, V.D., Walekar, L.S., Gore, A.H., Anbhule, P.V., & Kolekar. G.B. (2016). Spectroscopic analysis on the binding interaction of biologically activepyrimidine derivative with bovine serum albumin. **J Pharm Anal**, 6, 56-63.

Tamura A., Sugimoto K., Sato T., & Fujii T. (1990). The effects of haematocrit, plasma protein concentration and temperature of drug-containing blood in-vitro on the concentrations of the drug in the plasma. **J Pharm Pharmacol**, 42, 577-580.

Tan, H., Chen, H., Ma, L., Liu, S., Zhou, H., Zhang, Y., Guo, T., Liu, W., Dai, H., & Yu, Y. (2019). Fluorescence Spectroscopic Investigation of Competitive Interactions between Quercetin and Aflatoxin B_1 for Binding to Human Serum Albumin. Toxins (Basel) 11, 214.

Yan, J., Wu, D., Ma, X., Wang, L., Xu, K., & Li, H. (2015). Spectral and molecular modeling studies on the influence of β-cyclodextrin and its derivatives on aripiprazole-human serum albumin binding. **Carbohydrate Pol**, 131, 65-74

Yeates, K., Lohfeld, L., Sleeth, J., Morales, F., Rajkotia, Y., & Ogedegbe, O. (2015). A global perspective on cardiovascular disease in vulnerable populations. **Can J Cardiol**., 31, 1081-1093.

Zhang, W., Wang, F., Xiong, X., Ge, Y., & Liu, Y. (2013). Spectroscopic and molecular docking studies 668 on the interaction dimetridazole with human serum albumin. **J Chil Chem Soc**, 58, 1717- 669 1721.

Zhou, X.-Q., Wang, B.-L., Kou, S.-B., Lin, Z.-Y., Lou, Y.-Y., Zhou, K.-L., & Shi, J.-H. (2019). Multi-spectroscopic approaches combined with theoretical calculation to explore the intermolecular interaction of telmisartan with bovine serum albumin. **Chem Phys**, 522, 285–293.

Zhu, A.-P., Yuan, L.-H., Chen, T., Wu, H., & Zhao, F. (2007). Interactions between N-succinyl-chitosan and bovine serum albumin. **Carbohydr Polym**, 69, 363–370.